

Confocal Imaging Through Scattering Media with a Volume Holographic Filter

Michal Balberg⁺, George Barbastathis*, Sergio Fantini[%] and David J. Brady

University of Illinois at Urbana-Champaign, Urbana, IL 61801

* Massachusetts Institute of Technology, Cambridge, MA 02139

% Tufts University, Medford, MA 02155

ABSTRACT

The use of a volume holographic filter as collector element in a confocal system imaging through scattering (turbid) material is described. We show that the penetration depth of the volume holographic system is de-coupled from the scatter noise discrimination properties, and is potentially more advantageous than the traditional confocal microscope. Since the volume-holographic filter is a matched-filter, the penetration depth is dependent on the mismatch of the refractive index of the sample being imaged relative to the recording conditions. We present a method to overcome this limitation based on using a pre-compensating index matching film during the recording of the volume hologram. An improvement of the penetration depth is shown experimentally.

Keywords: confocal microscopy, volume holography, imaging through turbid media.

1. INTRODUCTION

Confocal microscopy with volume holographic collector was introduced in reference 1 as a new method for achieving optical depth sectioning. The volume hologram replaces the pinhole as a depth-selective optical filter. In this paper, we are interested in the application of the **volume holographic confocal microscope (VHCM)** to the problem of imaging through scattering (turbid) media, e.g. human tissue. We first describe the principle of operation of the VHCM, then we discuss the improvement that a pinhole-free operation is likely to introduce in the performance of the instrument when imaging through turbid media. We present experimental results supporting this point of view and discuss their implementation for imaging applications.

1.1 Confocal microscopy with a volume holographic collector

In the scanning confocal microscope, the field of view of the collector is reduced to a single point by placing a pinhole in front of the detector. The pinhole acts as a depth-selective filter, since it allows in-focus light to reach the detector and rejects light that is out-of-focus. The filtering operation of the pinhole is not matched to the response of any optical system in particular. As a result, a difficult trade-off arises in the design of pinhole-based confocal systems: if the pinhole size is reduced in order to improve depth resolution, the intensity of light that can reach the detector is severely limited resulting in loss of SNR (and, subsequently, loss in resolution). The opposite happens if the pinhole aperture is opened up in order to admit more light at the expense of depth resolution. The coupling of light budget and depth resolution is a direct consequence of the *ad hoc* nature of the pinhole filtering characteristics. It is natural, therefore, to consider whether another optical element may perform the depth filtering operation such that the trade-off does not arise; for this to happen, the filter must be matched to the point-spread-function (PSF) of the system.

In the VHCM, the phenomenon which leads to depth discrimination is the Bragg selectivity of volume holograms. Therefore, the volume hologram replaces the pinhole as a depth-selective element. At the same time, the volume hologram is a natural matched filter; it “remembers” the propagation properties of the beams that recorded it. Because the hologram is a wavefront selecting filter rather than a spatial filter, an efficient hologram does not limit the intensity of light passing

⁺ Correspondence: Email: mbalberg@uiuc.edu, gbarb@mit.edu

through. This observation justifies the ability of the volume hologram to select depth independently of its light-gathering properties.

More specifically, consider the recording geometry of Figure 1a. The volume hologram is recorded by the interference of two plane wave beams, one of which results from collimating light reflected from a surface at a reference depth. After recording is complete, the volume hologram is used as imaging element in the imaging geometry of Figure 1b. If the probe beam originates from the same reference surface that was used in recording the hologram, the reconstruction is Bragg matched, and the diffracted beam has maximum power (equal to the power of the probe beam times the diffraction efficiency). If the probe beam originates from a defocused surface, it fails to Bragg match the hologram, and as a result the diffracted power drops. An experimental curve of depth selectivity of the volume hologram is given in Figure 2a (bare silicon curve). The theoretical full-width-at-half-maximum (FWHM) of this curve is given by:

$$\delta_{FWHM} = 1.09 \times \frac{\lambda}{(\text{NA})^2}, \quad (1)$$

where λ is the wavelength, and (NA) is the numerical aperture of the collecting lens (L1 in Figure 1), corresponding to the angle of acceptance of the probe beam by the hologram. Note that the FWHM (which is a measure of depth selectivity) is not a function of the light gathering efficiency of the instrument; the latter is only determined by the diffraction efficiency of the volume hologram. By contrast, in traditional confocal microscopes the FWHM depends on the pinhole size², and, hence, the SNR of the optical system.

1.2 Penetration depth in scattering media

In reflection confocal microscopy, one is usually interested in detecting the light reflected from structures embedded at different depths inside an object. The useful penetration depth of light propagating in tissues is limited by the ability to detect the reflected, ballistic photons from the deep structures. The number of photons that reach the detector depends on the absorption and scattering coefficients of the medium and on the reflectance of the embedded structures. In a conventional-confocal microscope, this number is also limited by the diameter of the pinhole. For small pinholes, it was shown⁴ that the penetration depth is limited by the signal-to-noise-ratio (SNR) of the detecting system. In order to increase the flux of photons, the aperture can be increased. However, this results in broad depth discrimination (or a poor axial resolution) and in the collection of light scattered into the focal volume. As a result the penetration depth, for relatively large pinholes³ is limited by the loss of image contrast due to poor rejection of the background scattered light. In general, the penetration depth of a confocal microscope with a small pinhole is larger than that obtained with a large pinhole⁴.

As explained above, for a volume-hologram, the rejection efficiency of light reflected or scattered from points outside the focal volume is independent of the SNR of the system. Thus, assuming a system with a fixed SNR, the penetration depth of the volume holographic filter should be larger than that obtained with a small pinhole. Moreover, since the holographic filter is a matched-filter, the rejection efficiency of light scattered into the focal volume from outside is improved.

2. EXPERIMENTAL RESULTS

We carried out a series of experiments, to determine the penetration depth of the VHCM for imaging through scattering media. Since the volume hologram is a matched filter, a mismatch in the index of refraction of the scattering film, relative to the recording conditions, reduces the signal diffracted by the hologram. Recording with a bare silicon wafer allowed imaging a reflective surface through 430 μm of a scattering film with a reduced scattering coefficient (μ'_s) of 5 cm^{-1} . Thicker samples could not be resolved. In order to compensate for the index mismatch the holographic filter was recorded with a pre-compensating, index matching film. A 860 μm thick transparent polymer was used for recording, and reflection could be detected from a surface embedded in a 860 μm scattering film.

A volume holographic filter was recorded with an experimental setup similar to the one described in reference 1. The holograms were recorded in a LiNbO₃:Fe crystal, by illuminating with two plane waves oriented at a 90 degree angle. Figure 1 shows the experimental setup for recording and imaging. The 488 nm line of an Argon-Ion laser was used in this experiment. The reference beam is reflected from the surface that is being imaged. During recording the reference surface was positioned at the focal plane of the objective lens (L1), as a result the reflected beam is re-collimated by L1 before illuminating the crystal. Therefore the hologram is recorded with 2 plane waves. L1 used in this experimental setup has a magnification of 16x and a numerical aperture of 0.32, in order to achieve a larger depth of focus than can be obtained with high numerical aperture microscope lenses. This results in a broader depth sectioning resolution than the one presented in

reference 1. During reconstruction (imaging) the reference surface was scanned by a high-precision translation stage in the direction parallel to the optical axis of the reference beam (z-axis). In Figure 1a, a pre-compensating transparent polymer is placed on top of the silicon wafer during recording. In Figure 1b, the signal beam is blocked, and a scattering polymer is placed on top of the wafer for imaging through scattering media.

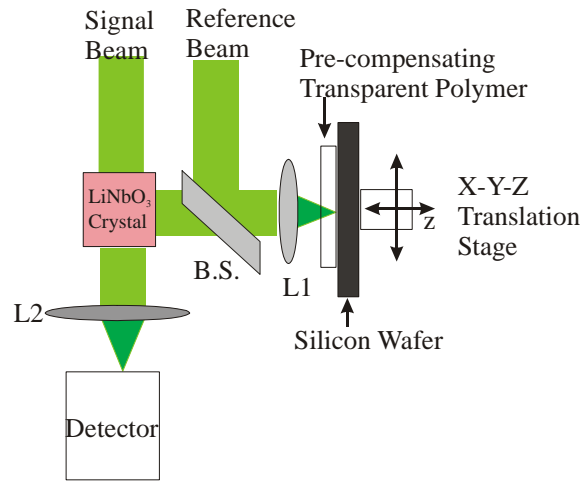


Figure 1a: Experimental setup for recording a volume holographic filter. L1, focusing lens for imaging the silicon wafer, L2, focusing lens of signal onto the detector, B.S. beam splitter.

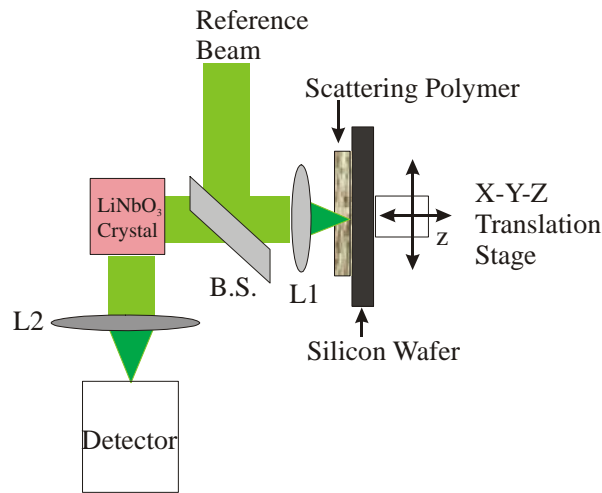


Figure 1b: Experimental setup for imaging through a scattering film placed on top of the silicon wafer being imaged.

The scattering samples were prepared as follows: Transparent films (marked with T) were made by curing rubber Silicone (GE Silicones RTV 615) at different thicknesses. Scattering films were made by mixing white Silicone (GE Silicones RTV 11) into the transparent rubber Silicone before curing. Two different concentrations of scatterers were mixed, a low scattering film (marked S1) with a reduced scattering coefficient (μ'_s) of $\sim 1 \text{ cm}^{-1}$, and a higher scattering film (S2) with $\mu'_s \sim 5 \text{ cm}^{-1}$. These values of the reduced scattering coefficients are comparable to those of soft tissues in the near infrared.

The diffraction efficiency was normalized by subtracting the minimum signal obtained in each scan from the data and dividing by the maximal signal (i.e. $(\text{Signal} - \min(\text{Signal})) / (\max(\text{Signal}) - \min(\text{Signal}))$, where Signal is a vector composed of the data points in one scan). This normalization method is used to stretch the contrast of the selectivity curves to full scale. It should be noted that for the higher scatterers, the relative noise level is higher than in the case of the low scattering films due to a lower intensity of the signal.

The experiment consisted of two parts. In the first set, the reference surface during recording was a bare silicon wafer. Imaging was performed through scattering films with different thicknesses, placed on top of the wafer. Figure 2a shows the normalized diffraction efficiency as low scattering (S1) films were placed on top of the silicon wafer during imaging. Since the scattering is low, there is hardly any difference in the normalized depth sectioning of the holographic filter for thin films (215 and 430 μm thick) when compared to the Bragg matched reconstructions (with a bare silicon wafer). Figure 2b shows the normalized diffraction efficiency through higher scattering films (S2). As can be seen, the graph of a film of 430 μm is very noisy. No signal could be resolved for S2 films thicker than 430 μm . The relative signal attenuation (due to the presence of the scatterer) was measured by comparing the maximal signal (*i.e.*, the signal measured with the surface in-focus) obtained when a 430 μm -thick film is placed on the wafer with the maximal signal for the bare silicon. It was found to be 10 times lower than a bare silicon in the case of S1, and 2,450 times lower in the case of S2. In both measurements, the same hologram was used, with diffraction efficiency approximately 2.5%.

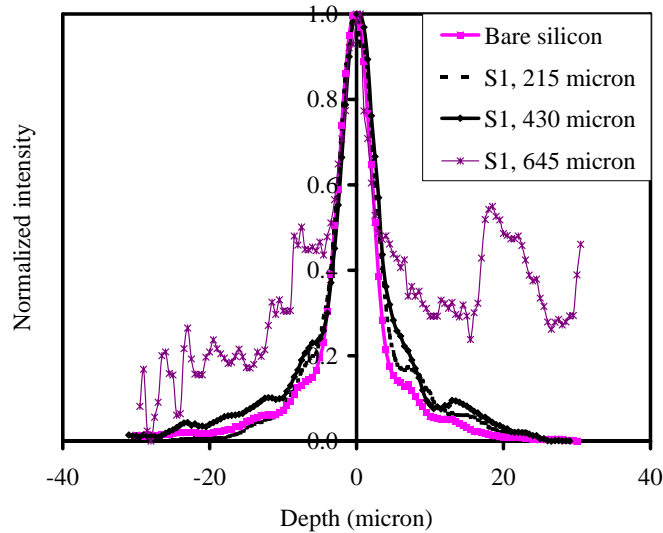


Figure 2a: Normalized signal vs. position of the silicon wafer for imaging through low scattering films (S1), at different thicknesses. The holographic filter was recorded with a bare silicon wafer at the focal plane of lens L1 (Figure 1a).

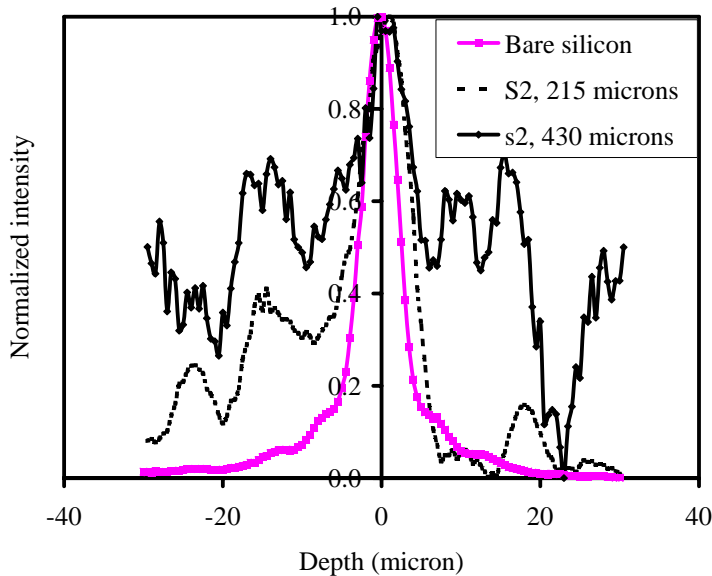


Figure 2b: Normalized signal vs. position of the silicon wafer for imaging through higher scattering films (S2), at different thicknesses. The holographic filter was recorded with a bare silicon wafer at the focal plane of lens L1 (Figure 1a).

In the second set, the holograms were recorded with a pre-compensating transparent film placed on top of the silicon wafer during recording (as shown in Figure 1a). The thickness of the transparent film was matched to the thickness of the scattering films placed during the imaging stage. In Figure 3a we plot the normalized diffracted signal obtained by recording with a pre-compensating transparent film (430 μm thick) and imaging through a T, S1 and S2 films of the same thickness. In Figure 3b the hologram was recorded while a 860 μm thick T film was placed on top of the wafer, and 860 μm thick T and S2 films were placed during imaging. The reflecting surface could be resolved through the thick scatterer, with a signal attenuation of 5.5 and 600 fold, respectively, for the S1 and S2 430 μm -thick scattering media. For the thicker 860 μm S2 scatterer the attenuation was measured at 700. Both measurements in this case are with respect to the silicon wafer surface in focus and covered with a transparent polymer of thickness 430 μm and 860 μm , respectively, which matches the recording conditions of the hologram.

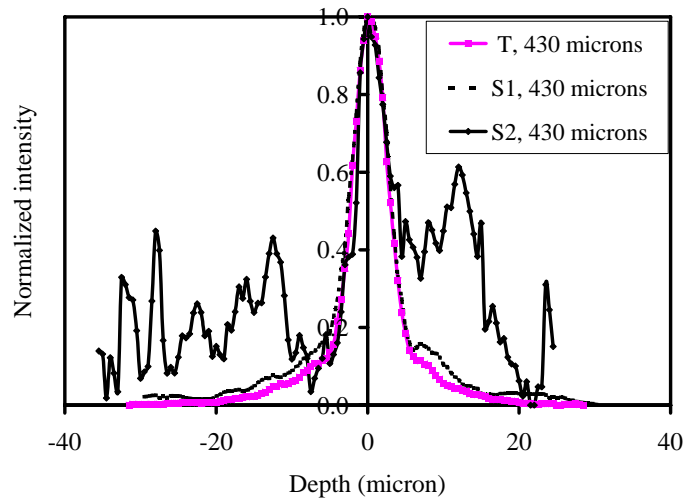


Figure 3a: Normalized signal vs. position of the silicon wafer for imaging a silicon wafer through a low scattering film (S1), and a higher scattering film (S2), thickness of 430 μm . The holographic filter was recorded with a transparent (T) film, 430 μm thick, placed on top of silicon wafer at the focal plane of lens L1 (Figure 1a).

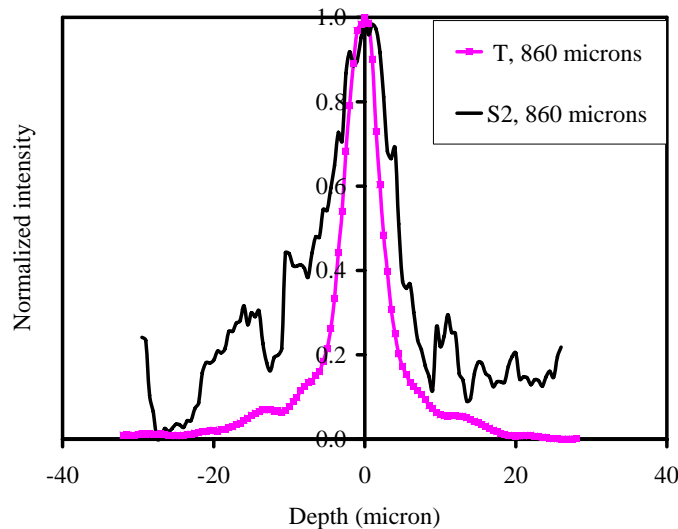


Figure 3b: Normalized signal vs. position of the silicon wafer for imaging a silicon wafer through a higher scattering films (S2), thickness of 860 μm . The holographic filter was recorded with a transparent (T) film, 860 μm thick, placed on top of silicon wafer at the focal plane of lens L1 (Figure 1a).

3. DISCUSSION

The volume hologram shows relatively high tolerance to the presence of a scatterer in the collection path. If the hologram is recorded with a bare silicon surface and reconstructed with the surface covered by a variety of scattering polymers (1st set of experiments), the tolerance to the scatterer is relatively low, and the signal drops to noise level for high-scattering high-thickness conditions. On the other hand, if the polymer is recorded with a pre-compensating layer of transparent polymer (2nd set), it becomes more tolerant to the presence of a scatterer mixed into the same polymer during imaging. In the experiments shown here, the scatterers were of the same thickness as the transparent pre-compensator. However, we recently obtained experimental evidence (not shown in this paper) that scatterers of lower thickness can also be imaged with small signal degradation using the pre-compensated hologram.

These results suggest that the penetration depth of the hologram is not limited by scatter noise, but rather by Bragg mismatch introduced due to the presence of the scatterer in a dielectric medium. A major contribution to the Bragg mismatch comes from the aberrations (primarily spherical) introduced in the path of the beam reconstructing the hologram; these reduce the peak diffraction efficiency and broaden the selectivity curve. The pre-compensator (transparent polymer used during recording) incorporates these aberrations into the hologram; during the imaging operation, the matched-filter character of the hologram phase-conjugates the aberrations out, thus improving the overall performance of the system.

REFERENCES

1. G. Barbastathis, M. Balberg and D.J. Brady "Confocal Microscopy with a Volume Holographic Filter", *Optics Letters*, 24(12): 811-813, 1999
2. T. Wilson, *Confocal Microscopy*, pg. 93-99, Academic Press Inc., San Diego, 1990.
3. M. Kempe, W. Rudolph and E. Welsch *J. Opt. Soc. Am A* **13**, 46-52, 1996.
4. C.L. Smithpeter, A.K. Dunn, A.J. Welch and R. Richards-Kortum *Applied Optics* **37**, 2749-2754, 1998.